Microelectronic Engineering 97 (2012) 122–125

Contents lists available at SciVerse ScienceDirect

Microelectronic Engineering

journal homepage: www.elsevier.com/locate/mee

Flexible resistive switching memory devices composed of solution-processed GeO_2:S films

Isaac Chung [a], Kyoungah Cho [b,*], Junggwon Yun [b], Sangsig Kim [a,b,*]

[a] Department of Nano Semiconductor Engineering, Korea University, Seoul 137-701, Republic of Korea
[b] Department of Electrical Engineering, Korea University, Seoul 137-701, Republic of Korea

ARTICLE INFO

Article history:
Available online 6 June 2012

Keywords:
ReRAM
Doped GeO_2
Unipolar
Flexible memories

ABSTRACT

In this study, resistive random access memory (ReRAM) devices are fabricated using solution-processable sulfur-doped GeO_2 (GeO_2:S) on flexible substrates. The Al/GeO_2:S/Au ReRAM devices exhibit the unipolar resistive switching behavior with an on/off ratio of more than 10^7 and the memory characteristics are retained after 10^4 s. The memory characteristics are unaffected by strains, even after the continuous substrate bending test for 10^3 cycles.

1. Introduction

Flexible resistive random access memory (ReRAM) devices have recently received attention as one of the promising memories for bendable systems because their vertical structures are independent of the lateral strain [1–5]. Since the first report on flexible ReRAM devices made of solution-processed titanium oxide films, flexible ReRAM devices consisting of solution-processable resistive materials have been actively studied, but their memory characteristics have barely improved [6–9]. In order to improve their memory characteristics, advanced resistive materials are needed for the fabrication of flexible ReRAM devices using the solution method, which is the most suitable technique for plastic-based flexible devices, due to its low-cost and simple processes at low temperatures. Recently, doped resistive materials are emerging in high-performance ReRAM devices constructed on rigid substrates [10–12]. We attempt herein to fabricate high-performance flexible ReRAM devices using doped resistive materials and examine their memory characteristics. Herein, sulfur and germanium oxide (GeO_2) are employed in this study as a dopant and resistive material, respectively, to overcome the poor memory characteristics of ReRAM devices consisting of solution-processable GeO_2 alone [13].

2. Experimental procedure

Germanium (IV) ethoxide (99.99%, Aldrich) and thioacetamide (99.99%, Aldrich) were used as the precursors of sulfur doped GeO_2 (GeO_2:S). First, 0.12 g of thioacetamide dissolved in 10 mL of ethanol was mixed with 0.2 mL of aqueous ammonia and the mixed solution was stirred for 5 min. Then, 0.1 g of germanium (IV) ethoxide was added to the mixed solution and stirred for 1 h. The GeO_2:S powder obtained by centrifugation was re-dispersed in ethanol for the spin-coating. In this study, the ReRAM devices were fabricated on poly-ether-sulfone (PES) substrates. The top and bottom electrodes were patterned using a photomask consisting of crossbars with a width of 100 μm. After the re-dispersed GeO_2:S solution was spin-coated onto Au bottom electrodes, the GeO_2:S films were annealed at 120 °C for 10 min in an Ar atmosphere. The annealing condition of 120 °C for 10 min was adopted to show clearly the resistive memory characteristics of the GeO_2:S film. Then, Al top electrodes were formed on the GeO_2:S films by thermal evaporation. Additionally, in order to examine the effect of S-doping, we deposited Al/GeO_2/Au on the plastic substrate using GeO_2 powder (99.999%, Aldrich) under the same conditions.

The synthesized GeO_2:S powders were characterized through X-ray diffraction (XRD; Bruker, GADDS) and transmission electron microscopy (TEM; JEOL, JEM-2100F). The electrical characteristics of the Al/GeO_2:S/Au devices were measured with an HP4155C semiconductor parameter analyzer in air. The bending tests of the flexible ReRAM devices were performed with a homemade bending machine.

3. Results and discussion

The XRD pattern (a), TEM image (b), and energy dispersed X-ray (EDX) profile (b and c) of the GeO_2:S synthesized in this study are shown in Fig. 1. The XRD pattern matches well with the lines drawn on the base of the standard JCDPS card (85-0473) of GeO_2. The GeO_2:S nanoparticles are clumped together, as shown in the

* Corresponding authors at: Department of Nano Semiconductor Engineering, Korea University, Seoul 137-701, Republic of Korea (S. Kim). Tel./fax: +82 2 3290 3909 (K. Cho); tel.: +82 2 3290 3245; fax: +82 2 3290 3894 (S. Kim).
E-mail addresses: chochem@korea.ac.kr (K. Cho), sangsig@korea.ac.kr (S. Kim).

0167-9317/$ - see front matter © 2012 Elsevier B.V. All rights reserved.
http://dx.doi.org/10.1016/j.mee.2012.05.032

TEM image and all of the components of GeO_2:S are indeed detected by EDX; note that the other peaks present in the EDX profile originate from the use of the carbon replica technique in this work.

Fig. 2 shows the representative *I–V* characteristics of the Al/GeO_2:S/Au device, demonstrating its unipolar resistive switching behavior. The switchable state of the Al/GeO_2:S/Au device is obtained after the initial electrical forming occurs at about 4.4 V, as demonstrated in Fig. 2. Electrical forming refers to breakdown events corresponding to the formation of filaments between the electrodes [1–8,10]. After the initial electrical forming, the resistance state changes from the high-resistance state (HRS) to the low-resistance state (LRS) associated with the generation of filaments between the top and bottom electrodes. In the second sweep of the voltage, the LRS switches to the HRS at reset voltages of less than 1 V and the set process occurring in the third sweep is responsible for the re-generation of the ruptured filaments. The inset shows the resistive switching characteristics of the Al/GeO_2/Au devices. The gap between the set and reset voltages of the Al/GeO_2:S/Au device is larger than 2 V, while that of the Al/GeO_2/Au device is about 1 V. The operating characteristics of the Al/GeO_2:S/Au device are more reliable than those of the Al/GeO_2/Au device. And the ratio of the resistance in the HRS to that in the LRS of the Al/GeO_2:S/Au device is more than 10^7, whereas that of the Al/GeO_2/Au device is about 10^4. The superior resistive switching characteristics of the Al/GeO_2:S/Au device compared to those of Al/GeO_2/Au is obviously due to the doping of S ions. As reported in Refs. [10–12] by other research groups, the doped ions are responsible for enhancing the characteristics of ReRAM devices. To understand the conduction and switching mechanisms of the Al/GeO_2:S/Au device, the current–voltage (*I–V*) characteristic is fitted in the logarithmic plots in Fig. 2(b). The LRS clearly exhibits the Ohmic conduction behavior with a slope of ~1, which is ascribed to the formation of metallic conductive filaments during the set process. Al is also an oxidizable metal like Ag or Cu. During the electrical forming, Al cations, generated by dissolving metal at the anode, migrate through the GeO_2:S film under the high electrical field. Reduction at the cathode results in the formation of the metal filaments. The strong affinity of Au for sulfur confines the effective area of the Al filament at the GeO_2:S/Au interface. The Al filament formation at settled regions contributes to the improved memory characteristics. On the other hand, two conduction mechanisms are observed in the HRS; Ohmic conduction mechanism at low voltages and Poole–Frenkel emission mechanism at high voltages [14,15]. The Ohmic conduction that occurs in the HRS at low voltages originates from the existence of some remnant filaments, but the current transport in the HRS at high voltages is controlled by Poole–Frenkel conduction.

The resilience of the memory characteristics to strain is examined by comparing the resistances of the HRS and LRS as a function of the bent state (a) or number of bending cycles (b), as demonstrated in Fig. 3. In this study, the strain applied to the substrate is 1.2% which is estimated using the following equation [16].

$$\text{strain} = \frac{(\text{substrate thickness}) + (\text{total film thickness})}{2 \times (\text{bending curvature radius of the substrate})} \times 100,$$

where the thicknesses of the substrate, the GeO_2:S film, and the top and bottom electrodes are 200 μm, 30, 80 and 200 nm, respectively. The strain of 1.2% applied to the substrate is the maximum sufferable value of the device in this study. Practically, the 1.2%-strain corresponds to the 120° bending curvature radius of the substrate. Under the more severe strain than 1.2%, the device does not work appropriately. Changes within the margin of error are observed in the resistances of the HRS and LRS between the flat state and the tensile or compressive strained states. The strain-independent phenomenon can be explained by the vertical channel and the ductility

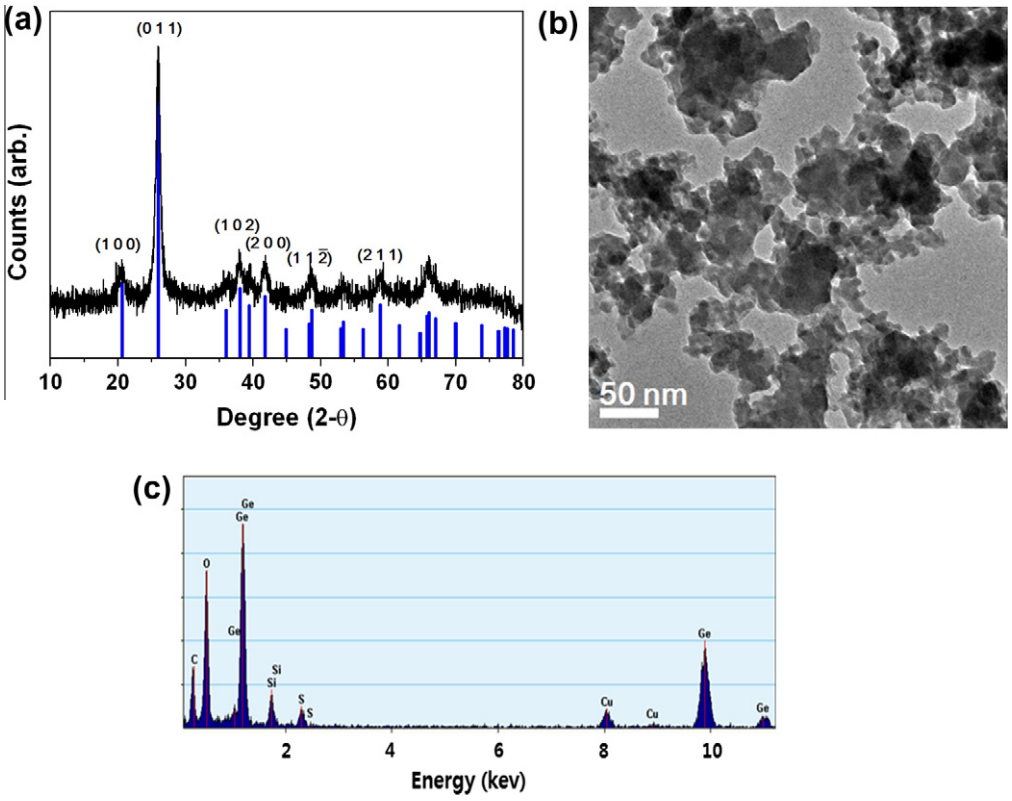

Fig. 1. (a) XRD pattern, (b) TEM image, and (c) EDX spectrum obtained from the synthesized GeO_2:S powders. The lines drawn on the base correspond to the standard JCPDS card (85-0473) of GeO_2.